8

The Behaviour of Low-Cost Passive Solar Energy Efficient House, South Africa

Golden Makaka*, Edson L. Meyer,
Sampson Mamphweli and Michael Simon
University of Fort Hare, Institute of Technology, Alice, South Africa

1. Introduction

A comfortable indoor environment is one of the main requirements of a well-designed house yet most of the low-cost houses are characterised by poor thermal performance. Mainly poor design, sub-standard building materials and poor craftsmanship contribute to the poor performance. The inclusion of energy-efficient passive solar design features in the construction of affordable housing offers many benefits which include; reduced operating costs, reduced energy related greenhouse emissions, and reduced need for expensive heating and cooling of the house and above all, improved comfort. The basic natural processes used in passive solar energy are the thermal energy flows associated with radiation, conduction, and natural convection. When solar radiation strikes a building, the building materials can reflect, transmit, or absorb the solar radiation [Makaka, Meyer; 2008]. Additionally, solar energy causes air movement that can be predictable in designed spaces. These basic responses to solar heat lead to design elements, material choices and placements that can provide heating and cooling effects in buildings. The thermal state is determined by the difference of the sums of the heat gains and heat losses. Bricks form the about 80% of the building materials and their physical properties play a role in determining the indoor thermal behaviour. These properties include thermal conductivity, water absorption, sound dumping and compressive strength. The addition of fly ash to clay in a defined ratio can really improves these properties and at same time reducing the manufacturing process. South Africa produces about 90 tones of fly ash annually posing a huge problem on the disposal management of fly ash. The use of fly ash in the manufacturing of bricks is one of the ways of the management of this waste.

The aim of this chapter is to establish the impact of passive solar design and building materials properties on the indoor temperature and to establish a statistical correlation of the indoor temperature with outdoor weather parameters [Makaka, Meyer; 2008]. It seeks to develop an understanding of the criteria used for the selection of an appropriate passive solar architecture that is sensitive to both energy use and climatic conditions, i.e., it gives the details of the design and the selection of building materials used, energy efficient design optimization using ECOTECT building design software and ventilation efficiency. Most of

* Corresponding Author

computer based prediction models are complicated for an average trained builder this results in the construction of poor thermal performing buildings. In this chapter a statistical method is used to develop a simple indoor temperature predicting model.

2. Principles of passive solar design

The building design phase integrates the site, floor plan, building orientation, landscaping, materials, mechanical systems and architectural characteristics. The design of an energy-efficient house requires a careful analysis and evaluation of all proposed design alternatives throughout the different design stages. The central issue in passive solar design is to minimize the energy required for heating, cooling and artificial day lighting. This can be achieved through the use of a range of different features that improve the building's thermal and lighting performance. The properties of the building materials vary and selection must be in accordance with the climate of specific regions [Makaka, Meyer; 2008]. The decisions of the architect and builders in the early stages of the design process are fundamental to a holistic approach in constructing a passive solar house (PSH). In the schematic design phase of the PSH, prior to making any sizing of windows, wall thickness, etc., decisions on broader issues such as building orientation and the appropriate spatial organization of the building must be made. As the design is developed, more accurate investigations are needed to obtain the appropriate size of building components based on design criteria and objectives that are determined at the outset. Passive solar design integrates several issues that can be rather contradictory; larger glazing to achieve solar gains can result in overheating, and an airtight building can produce bad indoor air quality [Wray *et al*., 1979]. These issues must be dealt with carefully by seeking the best balance between the passive solar design requirements and the budget. Consequently, in the Southern Hemisphere, the house must be oriented north to maximize the heat gain of the low north winter sun but eliminating the possible indoor solar radiation penetration in summer. The direction of the prevailing winds determined the layout of major outdoor features and the placement of windows to enhance optimal natural ventilation. The basic components of passive solar design are discussed in the following sections.

3. Advantages of energy efficient design features

A whole-house "system" approach to design and construction is the appropriate method of developing energy-efficient and sustainable houses. A system approach considers the interaction between the site, building envelope, mechanical systems, occupants, and other factors. This system recognizes that the features of one component of the house can greatly affect others. Energy efficient houses are more comfortable because of stable indoor temperature. The indoor humidity is better controlled and drafts are reduced. Energy-efficient houses protect the planet and offers greater fire safety. Energy efficient houses experience less condensation, which protects framing, windows and finish materials [Kunzel *et al*, 2003].

4. Fly ash bricks

Bricks of different proportions of clay and fly ash were molded and compressive strength, water absorption and thermal conductivity were measured. The amount of fly ash was

increased in steps of 10% (in volume). The clay-fly ash ratio which produced a brick with high compressive strength, low water absorption and low thermal conductivity was then used to mold bricks for the construction of a passive solar house. The ratio of 1:1 (clay : fly ash) was found to produce a brick with the ideal properties, i.e., low water absorption capacity, low thermal conductivity, high heat capacity, high compressive strength and high sound damping. Table 1 shows the chemical composition of fly ash collected from two different sites. The properties of fly ash bricks depend mainly on two factors: (i) the energy content of the fly ash used and (ii) the chemical composition of the fly ash [Makaka, Meyer, 2008]

Site	Sulphate (as SO_4^{2-})	Phosphate (as PO_4^{3-})	Silicate (SiO_2^{2-})	Calcium (Ca^{2+})	Magnesium (Mg^{2+})	Potassium (K^{+})	Aluminum (Al^{3+})
A	0.3	<0.1	20.3	0.36	0.05	1.63	14.1
B	0.2	0.1	20.9	2.15	0.12	2.68	19.6

Table 1. Percentage chemical composition of fly ash [Makaka, Meyer, 2008]

The other constituents include FeO, Na_2O, K_2O and unburnt carbon that form the bulk part of the fly ash. The South African fly ash has high-energy content, making it excellent for manufacturing bricks. Chemical composition of the fly ash and the temperature attained during burning determine the brick colour.

Figure 1 shows the variation of thermal conductivity with the increase percentage of fly ash in the brick composition, i.e., the insulating property of the fly ash brick increases with the increase of the amount of fly ash. The fly ash bricks are observed to have high heat making them ideal for use as thermal mass. From figure 1, it can be seen that thermal conductivity decreases with increase in the proportion of fly ash with a minimum value of about 0.0564 W/mK, which correspond to a mixing proportion of 50% fly ash to 50% clay by volume. The mixing proportion of 50% fly ash to 50% clay result in 93% reduction in thermal conductivity as compared to a pure clay bricks. The fly ash bricks are very light in weight (density 400-1190 kgm^{-3}) making it much easier to transport the bricks [Makaka, Meyer; 2008]. As the carbon in the brick burns the trace elements melts thus sintering the brick and at the same time small-unconnected cavities are created, giving the brick effective heat insulating properties (low conductivity). Above 50% of fly ash, the cavities start to decrease in size and number as the metallic elements starts to dominant, thus increasing the thermal conductivity of the brick. The fly ash bricks have an added advantage of being very smooth with an attractive colour thereby doing away with the need for external plastering and painting.

Water is associated with deterioration processes affecting masonry materials. Its presence within the interior pore structure of masonry can result in physical destruction if the material undergoes wet/dry or freeze/thaw cycles [Raman *et al*., 2001]. The freeze/thaw process is particularly damaging if the masonry material has high water absorption. The high water absorption results in high expansion and contraction thus weakening the brick. Because of these factors, the water permeability of a masonry material is related to its durability.

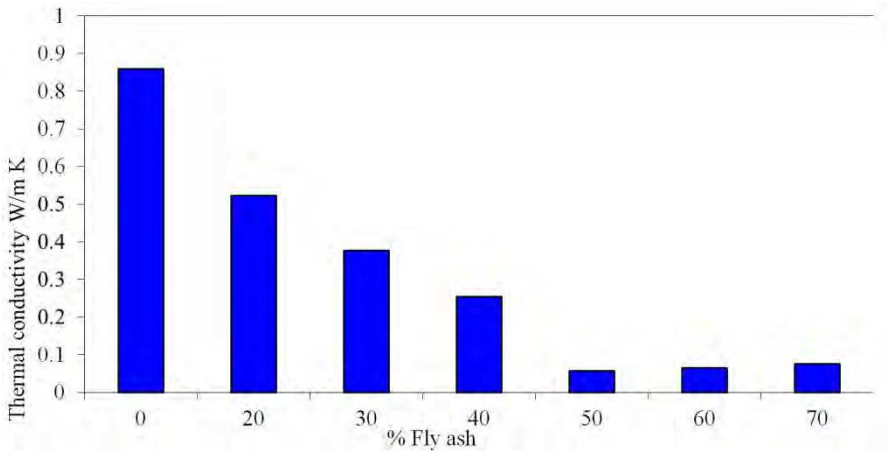

Fig. 1. The variation of thermal conductivity.[Makaka, Meyer; 2008]

Figure 2 shows the variation in water absorption as the amount of fly ash in the brick increases. Water absorption of fly ash bricks decreases with increase in fly ash. A mixing proportion of 50% fly ash to 50% clay produces a brick with minimum water absorption. According to the South African Building Standard Code (SABSC), the brick water absorption must be less than 20% by weight [Agrement South Africa, 2002].

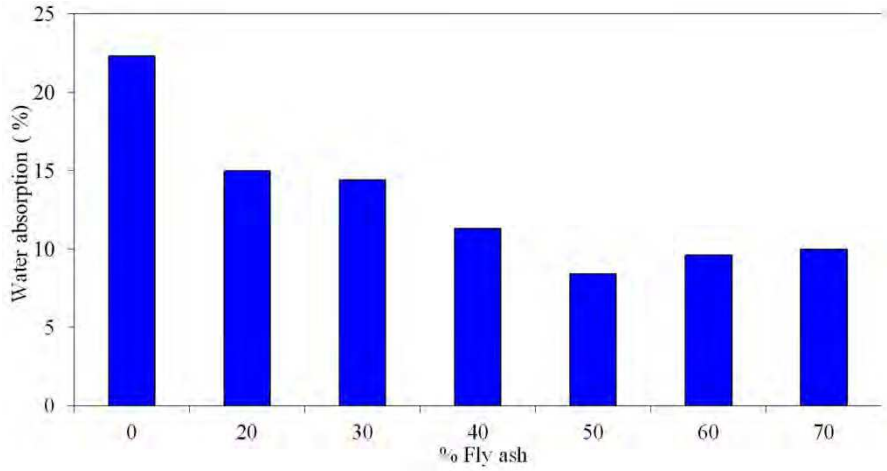

Fig. 2. Water absorption of fly ash bricks [Makaka, Meyer; 2008].

From figure 2 it is clear that the addition of 20% fly ash by volume reduces the water absorption by 32%, while the addition of 50% fly ash lowers the water absorption by 62%. Since the created cavities are unconnected, permeability and porosity are reduced. The reduction in permeability and porosity implies the reduction in freezing/thawing damage of the brick since there will be minimal amounts of water in the brick. As the content of fly ash increases beyond 50%, the amount of unburnt carbon increases and upon burning a

significant proportion of the brick will be burnt [Makaka, Meyer; 2008]. In this case the trace metallic elements are insufficient to bind the remaining proportion thereby creating connected cavities, which results in high water absorption bricks with low compressive strength. During brick firing the unburnt carbon enhance the burning process raising the temperature higher thus initiating the vitrification process to take place.

Figure 3 shows the variation in compressive strength of fly ash bricks for different proportions of fly ash. The compressive strength generally increases in comparison to bricks manufactured without fly ash. The SABSC specify the minimum brick compressive strength of 5 Mpa [Agrement South Africa, 2002]. The addition of fly ash significantly improves the compressive strength. The mixing proportion of 50% fly ash to 50% clay produced a brick with the desired properties, i.e., high compressive strength (12 MPa), low water absorption (8.84%) and low thermal conductivity (0.0564 W/mK). Fly ash bricks with this mixing proportion (50% fly ash) were recommended for wall construction. These bricks were bought from a local brick maker approximately 600 m from the site of construction.

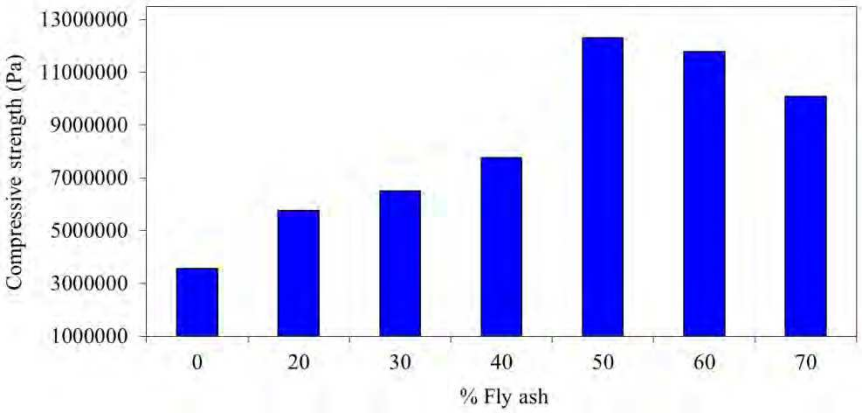

Fig. 3. Compressive strength of fly ash bricks [Makaka, Meyer; 2008].

Somerset East experiences high humidity, and there was need to use wooden doorframes and window frames which are resistant to rust. Being a poor heat conductor the wood minimizes the unwanted heat gain/loss. The wooden doorframes and window frames were found to have the added advantage of being cheaper than the metal frames. Corrugated iron sheets were selected for roofing as they were found to be much cheaper than other roofing materials such as roofing tiles. Asbestos was disregarded for health reasons since it causes asbestosis. Metallic purlins were selected based on strength; however they were not to protrude to the external. This was done to minimize heat/loss and fast corrosion.

5. Experimental passive solar house

5.1 Design of the passive solar house

A passive solar house was designed, simulated using Ecotect building design software and constructed on a land that slopes facing north with an average gradient of about 0.134, having good solar access, making it ideal for passive solar design. Figure 4 shows the transverse

section of the building. The design tried to harmonize the benefits of compactness and the requirements of natural day lighting, passive heating/cooling and natural ventilation. The sun's path determined the orientation of the house. The house was constructed to face north with more window area on the north wall to allow solar radiation penetration in winter to serve as solar heating thereby reducing the need of winter artificial heating. This orientation was to optimize the solar radiation that penetrates indoor in winter. The roof was split into two, the lower and upper roof. The lower roof faces north while the higher roof faces south.

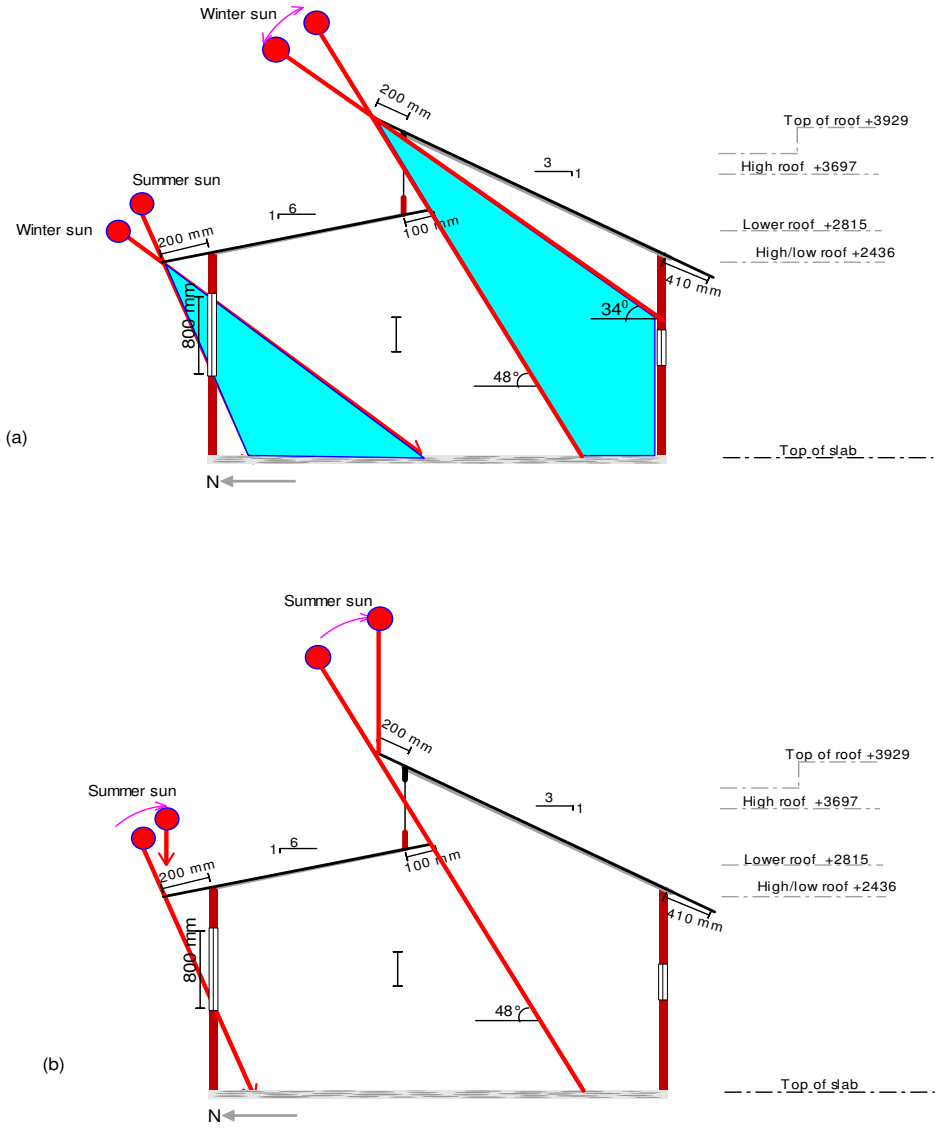

Fig. 4. Transverse building section: Solar radiation in (a) winter and (b) summer.

This was done in order to enable the insertion of clerestory windows making it possible to direct solar radiation to the desired rear zone (floor and southern wall) and to maximize day lighting, thus minimizing the use of electricity during the day. The northern roof is ideal for mounting photovoltaic modules as active solar energy converters.

5.2 Operation of the passive solar house

In summer, the sun almost rises from the east and sets in the west. In this case, the roof overhangs were made long enough (simulation was done ECOTECT) to eliminate the possibility of sunrays penetrating indoor. With reference to the clerestory windows, the upper roof was extended out by 200 mm while the lower roof was extended in by 100 mm. This eliminates the possible direct penetration of the solar radiation in summer while allowing maximum penetration in winter.

In winter (May to August) the sun rises almost northeast, but following a low northern path in the sky and then set in the northwest. From May to August the daily maximum angle of the sun ranges from 34° to 48° and this maximum angle occurs at around 12h15 with June 21st having the smallest angle. Thus, the north facing windows allows solar radiation to penetrate indoor, while the clerestory windows allow the south wall and the far south floor (thermal mass) to receive solar radiation. The thermal masses of high heat capacity (i.e. concrete floor of 100 mm thickness and the wall made from fly ash bricks) absorb solar radiation during the day.

The thermal masses used are of high heat capacity thus absorbing large amounts of solar energy with minimal temperature variation. This prevents overheating of the indoor environment, thus keeping the indoor temperature within the comfort levels. At night, as the outdoor temperature decreases; the thermal mass slowly radiates long-wave radiation heating the indoor air therefore keeping the indoor air temperature within the thermal comfort levels. Since the window glazes are opaque to the long wave thermal radiation, the thermal radiation emitted by the thermal mass is trapped indoor, and heat loses are minimized.

Somerset East experiences westerly prevailing winds in summer, so the small windows on the west and east make it possible to control the ventilation rate. The clerestory windows and the south windows enhance controllable natural ventilation rate and helps to maintain temperature within the comfort levels (16°C to 28°C).

6. Predicted performance of the passive solar house

The mathematical description of thermal behaviour of building systems is complex. It involves the modelling of several interconnected subsystems, each containing long-time constants, non-linearities and uncertainties such as convection coefficients, material properties, etc. Moreover, external unpredicted perturbations, i.e., external weather (e.g. temperature and humidity), soil temperature, radiation effects and other sources of energy, such as people, illumination and equipments, should also be taken into account.

The analysis of the different design alternatives was carried out by averages of an hourly dynamic simulation using Ecotect™ Building Design Software [Marsh, 2004]. Many building energy simulation software packages use the thermal zones concept to define thermal

properties for the simulation. The effects of building parameters on the façade thermal performance were studied through the simulations. Building models were built in the simulation program. The South African Building Standard Code specifies the lower and upper comfort levels to be 16°C and 28°C respectively and relative humidity levels of 30% to 60%.

Figure 5 shows the simulation results of the PSH. The simulation results indicate that the indoor temperature of the passive solar house was within the limits of the comfort levels for about 98% of the total period (380 hours) tested. However, the outdoor was outside the comfort levels for 44% of the period with 30% being above the upper comfort level (28°C) and 14% below the lower comfort level (16°C). With reference to figure 5, the PSH was observed to have an average thermal time lag of 3 hours and a decrement factor of 0.67.

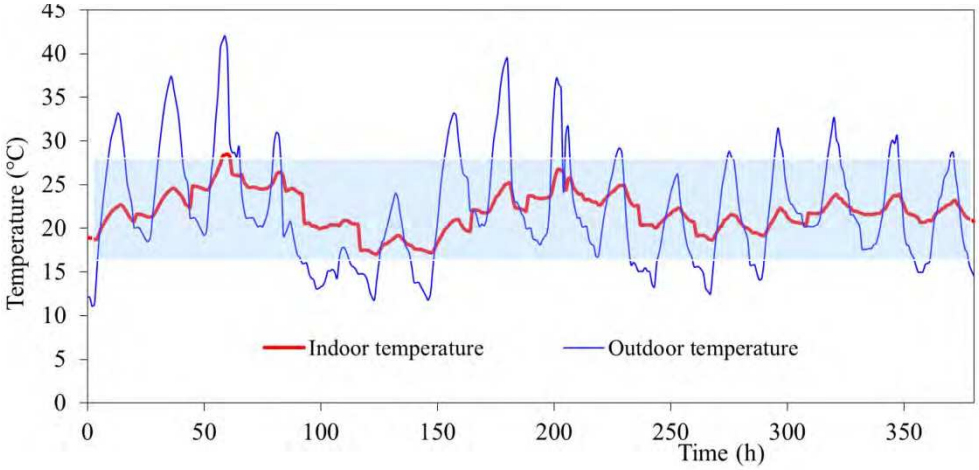

Fig. 5. Indoor and outdoor air temperature of the PSH simulated over a 380 h period (Summer).

The maximum indoor temperature attained was about 28°C and a minimum of 17°C giving a temperature swing of 10°C, while the outdoor temperature swing was about 31°C. However, it must be noted that the actual performance of the house is not only restricted to design and materials used, but also to the operation of the house on the part of the occupants.

7. Ventilation

7.1 Ventilation efficiency

Natural ventilation provides a cheaper and simpler way of cooling buildings. Low cost energy efficient passive solar buildings rely on natural ventilation and the building ventilation components must be positioned to capture the prevailing winds. Pollutants can build up to levels that may negatively impact human health unless they are removed or diluted with fresh outside air. The natural ventilation efficiency and air quality of the passive solar house was measured using the carbon dioxide tracer gas method. Reducing air leakage from the house envelope is one of the ways to reduce energy use, as well as improve

the comfort, health and building durability. Traditionally, residential construction greatly relied on air infiltration through the building envelope, i.e. through the unintended gaps in walls, roofs, windows, doors, and other construction elements to provide ventilation. Low cost energy efficient passive solar buildings rely on natural ventilation and the building ventilation components must be positioned to capture the prevailing winds [Myers, 2004].

House operation plays a key role in controlling a comfortable indoor environment. Somerset East experiences westerly prevailing winds (W (60 ± 15) N) and the passive solar house was designed to make use of these winds to control the indoor environment, i.e., indoor temperature and humidity, which are the key factors that determine thermal comfort. The South African Residential Ventilation Building Code [Agrement South Africa] recommends an average natural specific air exchange rate of 0.35 h^{-1} and an indoor carbon dioxide concentration less than 0.500%.

Equivalent outdoor airflow rate corresponds to the outdoor airflow rate that would result in the same CO_2 concentration in the measured room without inter-zone air flows.

An adult person produces on average (i.e. quiet or doing light work, about 100 W metabolic rate) carbon dioxide at about 20 *l/h*. At steady state, assuming that occupants are the only CO_2 sources, the equivalent airflow rate per person, Q_e, is related to CO_2 concentration (C_{in} indoors and C_{out} outdoors) by [Roulet, 1991]:

$$Q_e = \frac{S}{C_{in} - C_{out}} \ [m^3/h] \tag{1}$$

where S is the CO_2 source rate, i.e. about 20 l/h. Assuming a steady state (constant carbon dioxide concentration), equation 6.1 can be used to assess the equivalent outdoor airflow rate per person.

Another way is to use the CO_2 concentration records when there is no CO_2 source in the building. During these periods, the concentration decays down to the background concentration, by dilution with the outdoor air flow. If there is good mixing and if the outdoor air flow rate is constant, the decay is exponential and the factor corresponds to the air change rate and the concentration at any time t, is given as [Penman, 1982]:

$$C = C_0 e^{-\mu t} \tag{2}$$

where μ is the specific air exchange rate [h^{-1}] C_0 is the initial concentration above the background concentration. Taking logarithms both sides of equation 2 and differentiating with respect to time the specific air exchange rate can be approximated by the following expression:

$$\mu = -\frac{\Delta(In(C))}{\Delta t} \tag{3}$$

If the outdoor airflow rate is not constant, the decrement calculated from two measurements of concentration taken at time t_1 and t_2 provides an unbiased estimate of the average equivalent outdoor specific airflow μ.

7.2 Ventilation rate

Tracer gas tests were conducted over a period of time to measure actual air change rates. Figure 6 shows the indoor air currents due to the westerly prevailing winds. Carbon dioxide was injected into the house and its concentration monitored over time to determine how quickly the gas dissipates through the house's envelope. The west side ventilation components were used to control the indoor environment by regulating the amount of air flowing into the house. A carbon dioxide sensor was placed in the centre of the house at a height of about 0.45 m above the floor.

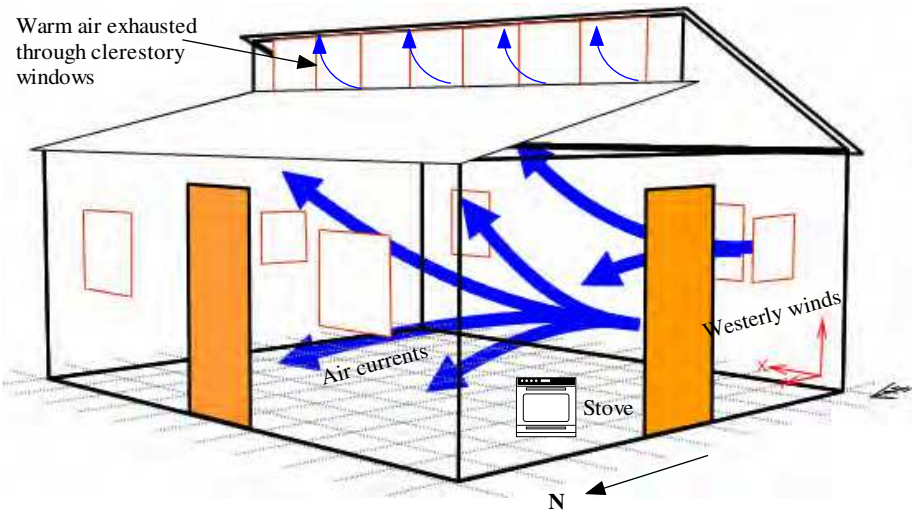

Fig. 6. Air current movements.

A fan was used to pump the indoor air into the sensor at a rate of about 300 *ml*/min. To investigate the effects of each of the ventilation component configurations, i.e., windows and doors, the ventilation rate tests were done in four configurations. A carbon dioxide sensor connected to a CR1000 datalogger and a computer was used to monitor carbon dioxide concentration in the house.

Configuration I

The carbon dioxide gas was injected into the house when all doors and windows were closed and a fan was used to mix the air in the house for about 5 minutes. The operation of the fan was intended as a contingency plan to evenly distribute the initial tracer dose throughout the space for the calculation of exchange rates. The *windows and doors were then opened* and carbon dioxide concentration was recorded at 1-minute time intervals until a constant concentration was achieved.

Configuration II

Carbon dioxide was injected into the house with doors and windows closed; a fan was switched on for 5 minutes to mix the air. *Windows were then opened but keeping the doors closed* and carbon dioxide concentration readings taken at 1-minute intervals.

Configuration III

The procedure of configuration II was repeated but *doors were opened and windows closed* and the carbon dioxide concentration recorded at a 1-minute intervals.

Configuration IV

The procedure cited in phase 2 was repeated but all *windows and doors were closed* and carbon dioxide concentration recorded at 1-minute interval.

In all the above cases it was not possible to inject equal amounts of the tracer gas as the equipment used could not allow the measurement of the amount of gas injected.

7.3 Ventilation rate

The tracer gas technique was used to measure the air exchange rate. Figures 7 and 8 illustrate the tracer gas concentration profiles measured for different ventilation component configurations, i.e., opening and closing of doors and windows. The average indoor and outdoor temperatures during these tests were, T_{in} = 20 °C and T_{out} =17 °C, and an average wind speed of 0.5 m/s blowing from W($60^0 \pm 15^0$)N. Figure 7 show the tracer gas concentration variation for configuration I, i.e., when both windows and doors were open. Results indicate that the concentration decays exponentially to the background concentration within a period of 16 minutes. Assuming that the west window and door are the only paths through which the westerly winds enter the house, then the mass air flow rate through the door and window is approximated by equation $\dot{m} = C_d A\sqrt{2\rho\Delta P}$. Taking the average air density to be 1.2 kg/m^3 and an average indoor and outdoor pressure difference of 4 Pa. For wide-open windows and doors, the opening area is the sum of the windows and doors areas, which gives 2.06 m^2, and taking the discharge coefficient C_d = 0.6, the average mass airflow was found to be approximately 3.83 kg/s.

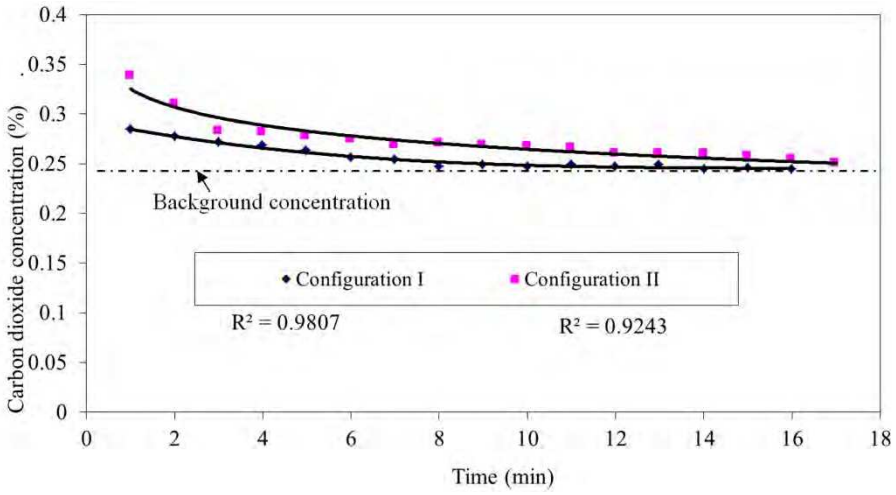

Fig. 7. Tracer gas concentration decay for configuration I and II [Makaka, Meyer; 2008].

From figure 7 it was observed that the closing of doors significantly reduced the carbon dioxide concentration decay rate implying a reduction in the ventilation rates achieved when both doors and windows were open. Opening windows and closing doors reduced the mass flow rate to 3.16 kg/s (i.e. a reduction of 17%). This means doors play a significant role in the ventilation of the PSH.

Figure 8 illustrates the decay of the tracer gas concentration for configurations III and IV, i.e., for open doors and closed windows, and for when both windows and doors were closed. Comparing configurations I and III it was found that the opening of doors and closing windows reduced the mass flow rate from 3.83 kg/s to 0.67 kg/s (i.e. a reduction of 82%). Configuration IV produced the minimum tracer gas concentration decay rate. It took approximately 69 minutes for the tracer gas to decay to the background concentration. When both doors and windows were closed, the infiltration and exfiltration airflow was through the unintended gaps, such as, gaps between floor and door, roof and wall, etc.

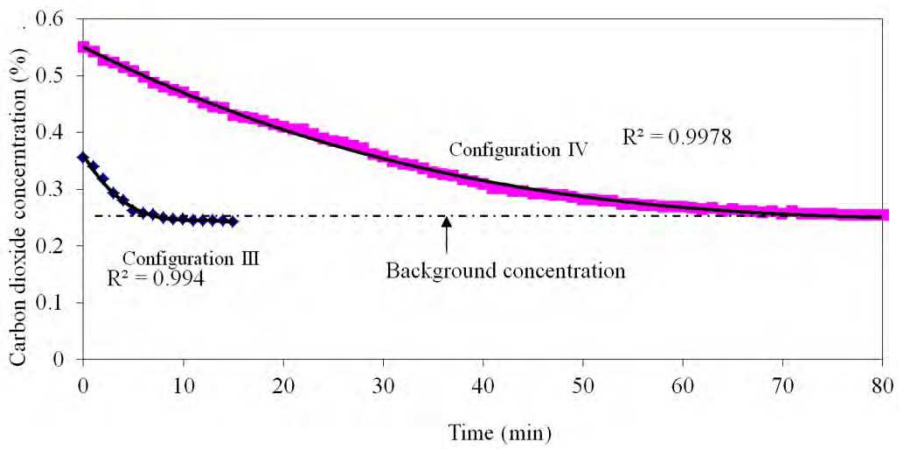

Fig. 8. Tracer gas concentration decay for configuration III and IV [Makaka, Meyer; 2008].

With reference to figures 7 and 8 and taking a reference initial tracer gas concentration of 0.28% the time taken for the tracer gas concentration to decay to the background concentration varied depending on the type of the ventilation components in use. Table 2 summarizes the time taken for the carbon dioxide concentration to decay from 0.28% to the background concentration. From Table 2 it can be seen that windows have a higher ventilation effect (shorter decay time) than doors. However this depends on the wind speed and direction and the orientation of the ventilation component with respect to the wind direction.

Somerset East experience W($60^0 \pm 15^0$)N prevailing winds, and when windows are open and doors closed, the west side windows capture the prevailing winds which then escape through the east and south windows, and to a lesser extent through the north side windows. This gives an effective controllable air inflow and outflow by adjusting the opening area of windows.

In the case where windows are closed and doors open, the west side door captures the prevailing winds. Since the prevailing winds are not purely westerly, components of the inflow air currents also penetrate through the north side door. These currents are then opposed by the inflow air current through the west side door which will try to escape though the north side door as it is the only designed escape path under this configuration. This results in reduced concentration decay time, implying a reduced air exchange rate as compared to when windows are open and doors closed.

Ventilation components state	**Decay period** (minutes)
Configuration I: All windows closed and doors open	16
Configuration II: All doors closed and windows open	17
Configuration III: All doors and windows open	13
Configuration IV: All windows and doors closed	69

Table 2. Decay periods for different ventilation components status.

7.4 Air quality

Several decay periods can be observed from figures 12 through 13. For each period, the initial and final times were determined and a normalized concentration, C_n, was calculated for each measurement time:

$$C_n = \frac{C(t) - C(0)}{C(0) - C_0} \tag{4}$$

where C(0) is the initial concentration at the beginning of the decay period and C_0 is the background concentration and was found to be 0.234%. This background concentration was first deducted from the carbon dioxide concentration to get the increase resulting from the instant of injection. Figures 9 and 10 show the graphs of $Ln(C_n)$ versus time for different ventilation component configurations. The air change rate, which is the slope of the line that represents $Ln(C_n)$ versus time was calculated for each graph.

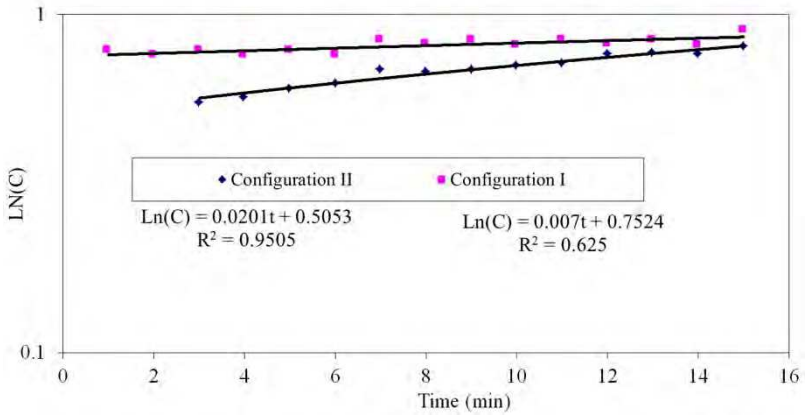

Fig. 9. Logarithmic graph of concentration: configuration I and II [Makaka, Meyer; 2008].

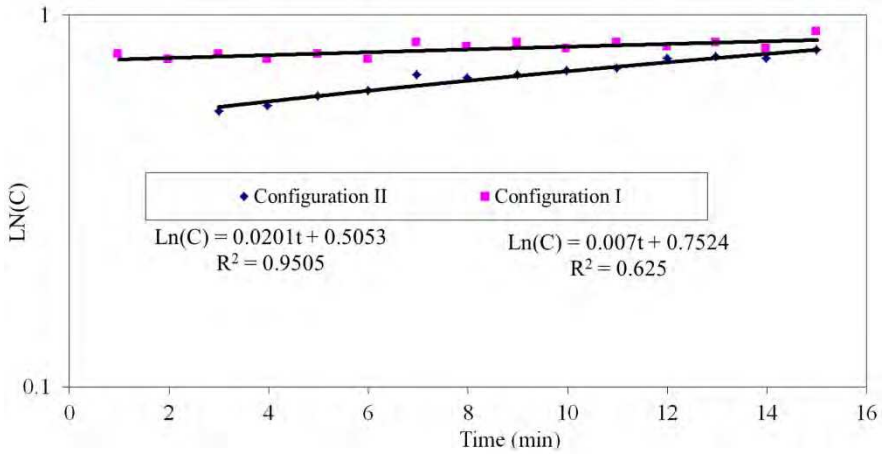

Fig. 10. Logarithmic graph of concentration: configuration III and IV [Makaka, Meyer; 2008].

Table 3 shows the calculated specific airflow exchange rates (μ) for different ventilation component configurations. In this table, the confidence intervals were calculated from the dispersion of the concentration measurements around the regression line, using 0.1% probability (99.9% confidence). When all the designed ventilation components were closed (configuration IV) the least specific air exchange rate (μ) of (0.29 ± 0.03) h^{-1} was observed as compared to other ventilation component configurations. The equivalent outdoor airflow rates (M_{eq}) for each ventilation component configurations were calculated using the expression: $M_{eq} = \mu V$, where V is the volume of the house. The house has a volume of 34.56 m^3 and an envelope area of 61.1 m^2. Assuming that the flows are due to the envelope leakage the specific leakage rate (S_L) was obtained using the expression: $S_L = \frac{M_{eq}}{A}$ where A is the area of the envelope and results are summarized in table 3

Configuration	Ventilation component status	Specific air exchange rate μ (h^{-1})	Equivalent outdoor air flow rate M_{eq} (m^3/h)	Specific leakage rate S_L ($m^3/h.m^2$)	Rate of ventilation heat flow Q_v (J/s)
I	Doors and windows open	9.58 ± 0.04	331.08 ± 1.38	5.42	772
II	Doors closed and windows open	1.74 ± 0.02	60.13 ± 0.69	0.98	140
III	Doors open and windows closed	0.84 ± 0.04	29.03 ± 1.38	0.48	68
IV	Doors and windows closed	0.29 ± 0.03	10.02 ± 1.04	0.16	24

Table 3. Specific airflow rates calculated from the various CO_2 concentration decays [Makaka, Meyer,; 2008]

The ventilation rate determines the indoor environment as the incoming air carries with it thermal energy. If the outdoor temperature is higher than the indoor, and as the outdoor air flows indoors, the tendency is to raise the indoor temperature. The rate of ventilation heat flow is approximated by equation. $Q_v = 1200 M_{eq} \Delta T$. Taking the average indoor-outdoor temperature difference ΔT to be 7°C and the ventilation rates from Table 3, the ventilation heat flow rates were calculated. Table 3 also shows the summary of results for the rate of ventilation heat flows for different ventilation component configurations. Depending on the indoor and outdoor temperature difference, configuration I, which has the highest rate of ventilation heat flow, can result in excess heat gains or losses. However, adjusting the effective open areas of the ventilation components can regulate the heat gain/loss, thus keeping the indoor environment within the comfort levels.

It must be noted that the rate of ventilation heat flow for configuration IV is through the unintended ventilation path ways, i.e. through gaps between doors and floors, etc, since all designed ventilation components were closed.

8. Indoor temperature variation

8.1 Prediction of indoor temperature

The mathematical description of thermal behaviour of building systems is a complex process. It involves the modelling of several interconnected subsystems, each containing long-time constants, non-linearities and uncertainties such as convection coefficients, material properties, etc. The indoor temperature is affected by a number of stochastic parameters, which include, wind speed and direction, relative humidity, solar radiation and outdoor temperature. The random infiltration rate and thermophysical properties (such as thermal conductivity of the walls and heat capacity of the room) have an impact on the indoor temperature.

The statistical approach allows estimating the probabilistic future thermal behaviour of buildings based on monitored statistical information, such as outdoor temperature, relative humidity, etc. The stochastic behaviour of the occupants in operating the ventilation components and other indoor human activities greatly affects the thermal performance of buildings. Some can even choose to close doors to avoid pets to get indoor thus compromising the thermal performance of the house. These parameters sometimes are uncertain and in some cases are difficult to find the exact information.

8.2 Correlating T_{in} and T_{out}

Figure 11 shows the best-fit linear regression correlations of the indoor and outdoor temperatures for summer. It was seen that the indoor and outdoor temperatures had different correlations for low temperatures (less than 28°C), and for high temperatures (greater than 28°C). At low temperatures the correlation factor was found to be $R^2 = 0.8064$ while for high temperatures the correlation factor was $R^2 = 0.6028$. At low temperatures the correlation was found to be stronger implying that at low temperatures there is less dependence on other parameters such as relative humidity as compared to high temperatures. At high temperatures relative humidity was found to be very low (minimum),

while the solar radiation was maximum. This suggests that relative humidity and solar radiation have significant influence on the indoor temperature at high outdoor temperatures. The peak indoor temperatures were found to occur during cooking periods and thus creating a departure from the low temperature variation trend. A departure of about 57% was observed from the low temperature variation trend to high temperature variation trend and this departure is indicated in figure 11 by a double arrow. This departure can be due to indoor heat sources, such as heat from stove. At low temperatures the correlation between the indoor and outdoor temperature was found to be:

$$T_{in} = 0.691T_{out} + 11.67 \tag{5}$$

while at high temperatures it was found to be:

$$T_{in} = 1.088T_{out} + 0.308 \tag{6}$$

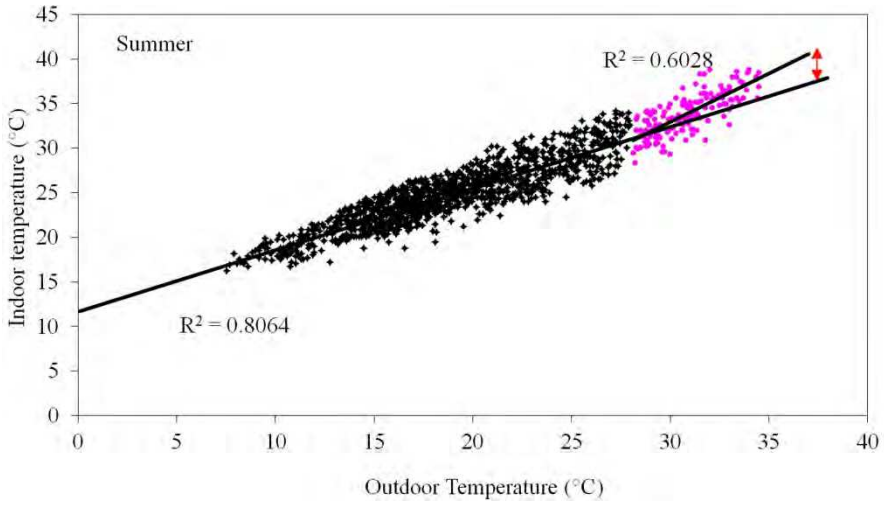

Fig. 11. Summer: Correlation of indoor and outdoor temperature [Makaka, Meyer; 2011].

Figure 12 shows the best-fit correlation of the indoor to the outdoor temperature for winter period. At high outdoor temperatures (above 28°C) the correlation factor was found to be $R^2 = 0.4568$ while at low temperatures (less than 28°C) it was $R^2 = 0.7391$. At low temperatures the correlation is relatively stronger than at high temperatures implying that the outdoor temperature has a greater influence on the indoor temperature at low temperatures. The departure from the low temperature variations trend was found to be about 62% and is indicated in figure 19 by a double arrow. This departure may be attributed to indoor heating and activities which are independent to the outdoor temperature.

At low temperatures the correlation function between the indoor and the outdoor temperature was found to be:

$$T_{in} = 0.657T_{out} + 8.671 \tag{7}$$

while at high temperatures it was found to be:

$$T_{in} = 1.052T_{out} + 1.449 \quad (8)$$

From the correlation functions for summer and winter it was observed that the outdoor temperatures have significant influence on the indoor temperature. It must also be noted that, if a change occurs in the comfort parameters (e.g., temperature) that might result in discomfort, occupants react in a way that tend to restore their comfort, and there is no precise temperature at which one opens a window, but as the temperature rises there is an increase in probability that windows need to be opened. In figure 12, a significant number of data points appear as outliers. Although the occupants never used a proper heater, it is highly likely that at times they used a two-plate electrical stove to heat the indoor environment, thus giving rise to outliers. It must be noted that the outliers are above the trend line, confirming that at times a heating system was used. However the occupants never reported the use of a heater or fan.

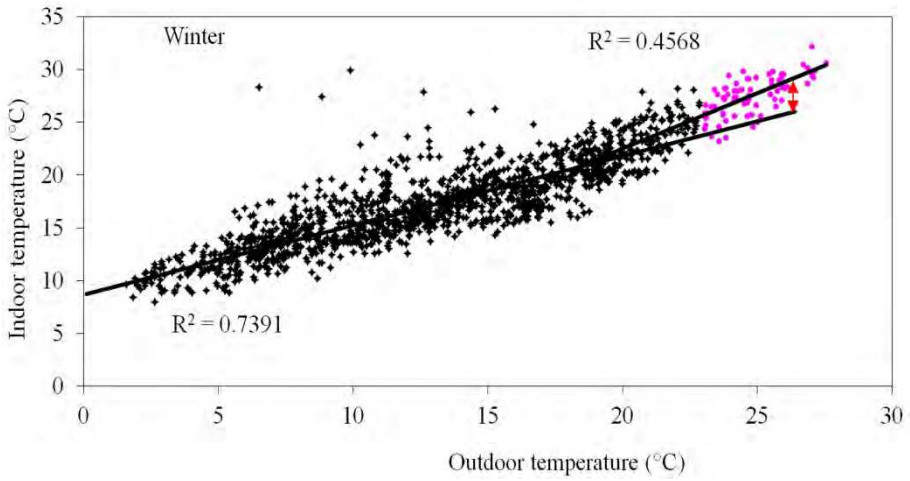

Fig. 12. Winter: Correlation of indoor and outdoor temperature [Makaka, Meyer; 2011].

The wide dispersion of the points about the trend line also indicates that the indoor temperature is not affected by the outdoor temperature only but by other factors such as ventilation rate, relative humidity, wind speed and solar radiation. The correlations also suggest that the passive solar house is freeze resistance since when the outdoor temperature is 0ºC, the indoor temperature would be about 8°C in winter and much higher (about 12°C) in summer. From the measured data it was observed that on the 29/5/29 at around 06h30 the outdoor temperature dropped to about 1.6°C and the indoor temperature only dropped to 9.4°C. This indicates the high heat retention capacity of the thermal mass (fly ash bricks), such that when the outdoor temperature drops to zero, the stored thermal energy in the wall continue to heat the indoor air keeping it at a temperature above 8°C.

8.3 Correlating T_{in} and outdoor relative humidity

Figure 13 shows the correlation of indoor temperature to outdoor relative humidity for summer. The data points were found to follow two distinct distribution trends, i.e., at low (less than 34%) and high (greater than 34%) relative humidity. The correlations factors were found to be very weak, for low relative humidity the correlation factor was found to be, $R^2 = 0.2774$ while for high relative humidity it was found to be $R^2 = 0.3099$. The differences in correlation strength at low and high relative humidity suggest that there are other variables which dominate at low relative humidity and not at high relative humidity. At low relative humidity solar radiation was found to have a greater influence on the indoor relative humidity variation. The low correlation factors indicate that there are other parameters which have a higher impact on the indoor temperature than the outdoor relative humidity. At low outdoor relative humidity (less than 34%) the correlation was found to be:

$$T_{in} = -0.3395(RH)_{out} + 40.464 \tag{9}$$

while at high relative humidity the correlation was:

$$T_{in} = -0.1184(RH)_{out} + 33.389 \tag{10}$$

Figure 14 shows the correlation of the indoor temperature and outdoor relative humidity for the winter period. The data points were found to be more scattered than for the summer. The high scatter is due to the variability of the Somerset East weather, which can change two to three times a day and a change of indoor activities due to the change of season. The dependence of the indoor temperature with the outdoor relative humidity was found to be different for low and high outdoor relative humidity. For low relative humidity the correlation factor was found to be $R^2 = 0.2657$ while for high relative humidity the correlation factor was $R^2 = 0.4027$. Low relative humidity was found to correspond to high temperatures, which is directly related to the solar radiation. High solar radiation was found to correspond to low relative humidity. At low relative humidity the correlation function was found to be:

$$T_{in} = -0.6862(RH)_{out} + 36.65 \tag{11}$$

while at high relative humidity the correlation function was found to be:

$$T_{in} = -0.1004(RH)_{out} + 22.70 \tag{12}$$

8.4 Effect of solar radiation on indoor temperature

Figure 15 shows the correlation of the indoor temperature and solar radiation. The correlation factor was found to be $R^2 = 0.5873$. It must be noted that the indoor temperature is affected by a number of factors, which include heat generated by the occupants and from equipments such as stove and refrigerator.

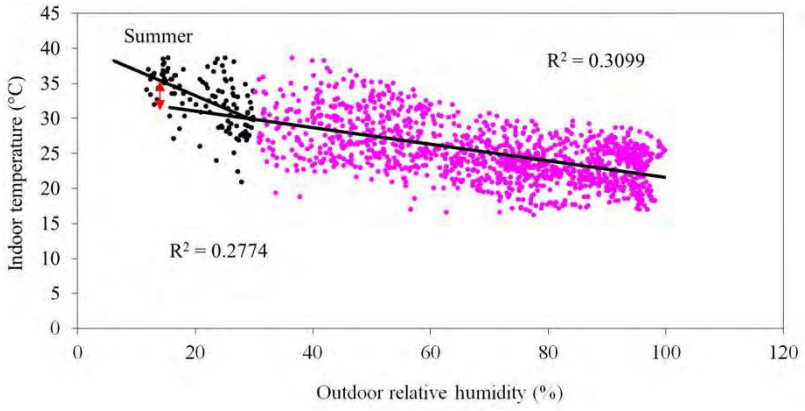

Fig. 13. Summer: Correlation of indoor temperature and outdoor relative humidity

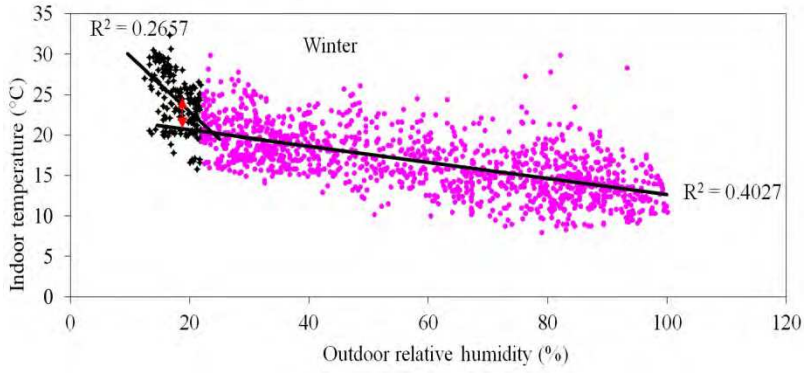

Fig. 14. Winter: Correlation of indoor temperature and outdoor relative humidity.

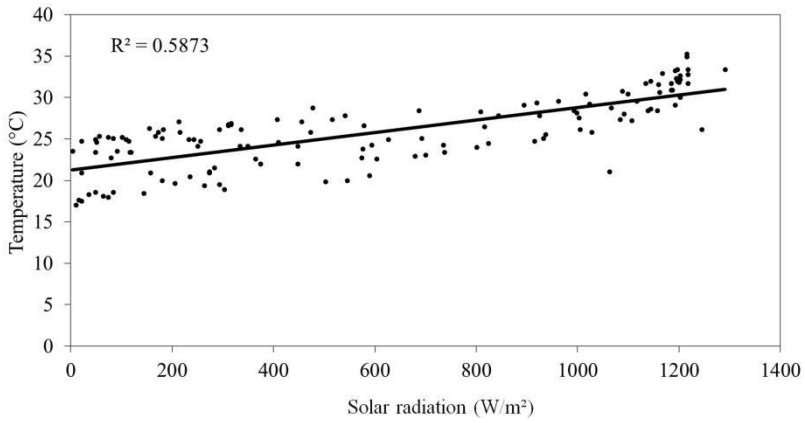

Fig. 15. Evolution of indoor temperature with solar radiation [Makaka, Meyer; 2011].

The indoor and outdoor temperature difference gives the direction of heat flow. High solar radiation was found to be associated with low indoor and outdoor temperature differences. Maximum indoor temperatures were found to occur at around 14h00. In summer the roof was found to attain high temperatures and the roof being of iron sheets (good thermal conductor) contributed significantly to the indoor temperature distribution. The high roof temperature diminishes the indoor and outdoor temperature difference. The correlation function between indoor temperature and solar radiation, I, was found to be:

$$T_{in} = 0.0075I + 21.27 \tag{13}$$

Equation (13) shows that when the solar radiation is zero (at night), the indoor temperature would be within the thermal comfort levels (about 21°C). During the day the thermal mass would have absorbed solar radiation and releases it at night thus keeping the indoor environment within the comfort levels.

8.5 Temperature modeling

The generalized mathematical model for predicting indoor temperature of any building has to take into account two types of data: on one hand the climatic conditions to which the building is exposed and, on the other hand, the thermal properties of the building. In an unoccupied house one can have a complete control over the conditions of the house, whether to open or close; shade or unshade the windows, etc. During the experimental period, the ventilation components can be maintained at the same configuration without indoor heat generation or cooling.

In occupied buildings the situation is very different, as the occupants have complete freedom to change the conditions according to their changing needs or desires. The activities of the occupants have a significant influence on the indoor temperature distribution. Predicting the indoor temperature is a very difficult and complex process, as random variables come into play, such as the closing and opening of the ventilation components. Outdoor weather variables such as wind speed, temperature, solar radiation and relative humidity are key determinant factors of the indoor temperature. However it must be noted that the indoor temperature is also linked to the heat fluxes generated in the house by appliances.

The performance of the house was observed to depend on how the occupants operate the house, and the thermal behaviour of the house in winter was seen to be different from that in summer. Based on the monitored results, the first stage in the development of the experimental predictive model was to analyze the patterns between (i) T_{in} and T_{out} (ii) T_{in} and I (iii) T_{in} and RH_{out} (iv) T_{in} and V_w. Taking into account these possible dependences predictive models for the indoor temperature for summer and winter were developed. A linear dependence was proposed as the above relation patterns were observed to be linear.

$$T_{in} = a_1 * T_{out} + a_2 * RH_{out} + a_3 * I + a_4 * V_w + a_5 \tag{14}$$

Where:

T_{in} = Indoor temperature
T_{out} = Outdoor temperature
V_w = Wind speed
I = Solar radiation
RH_{out} = Outdoor relative humidity
a_i = Regression coefficient

The constant a_5 takes into account heat generated indoors either by appliances or occupants. The above-proposed model is a simplification of a complex dependence. It must be noted that all the parameters involved are not independent. For example, the outdoor temperature greatly depends on irradiance and wind speed. Using regression analysis, the coefficients in equation (14) were determined.

For summer the following model was obtained:

$$T_{in} = 0.818207T_{out} + 0.013562(RH)_{out} - 0.12907V_w + 0.00038I + 8.18 \quad (15)$$

For winter the following model was obtained:

$$T_{in} = 0.898116T_{out} + 0.03914(RH)_{out} - 0.2545V_w + 0.00575I + 4.20 \quad (16)$$

Figures 16 and 17 show the comparison of the measured and predicted indoor temperatures for summer and winter, respectively.

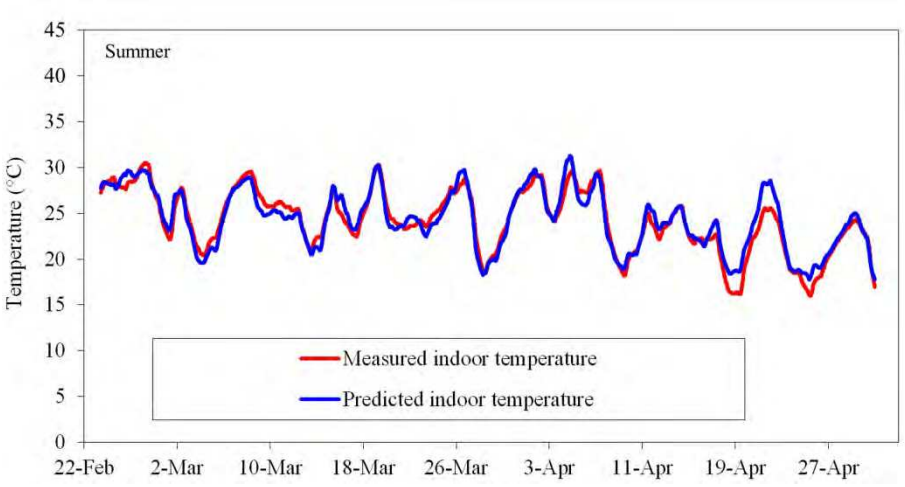

Fig. 16. Summer: measured and predicted indoor temperature [Makaka, Meyer; 2011]..

From equations (15) and (16) it can be noted that the outdoor temperature, solar radiation and outdoor relative humidity have a positive contribution to the indoor temperature, i.e.

when the outdoor temperature, solar radiation and relative humidity increase, the indoor temperature increases. But when the wind speed increases the tendency is to lower the indoor temperature. From the models it was seen that the outdoor weather parameters do have varying impact on the indoor temperature but with high sensitivity to the outdoor temperature. The determination of the sensitivity of the models revealed that the indoor temperature could be predicted to 85% accuracy in summer and to 87% accuracy in winter, considering the outdoor temperature only.

From figures 16 and 17, it can be seen that the predicted temperatures agree well with the measured data, however in summer there were some significant differences at some peak temperatures, with the measured temperature being higher than the predicted. These peak temperature differences were due to the indoor heat generating activities such as cooking and ironing. It must be noted that in the model thermal properties of the building were not taken into consideration.

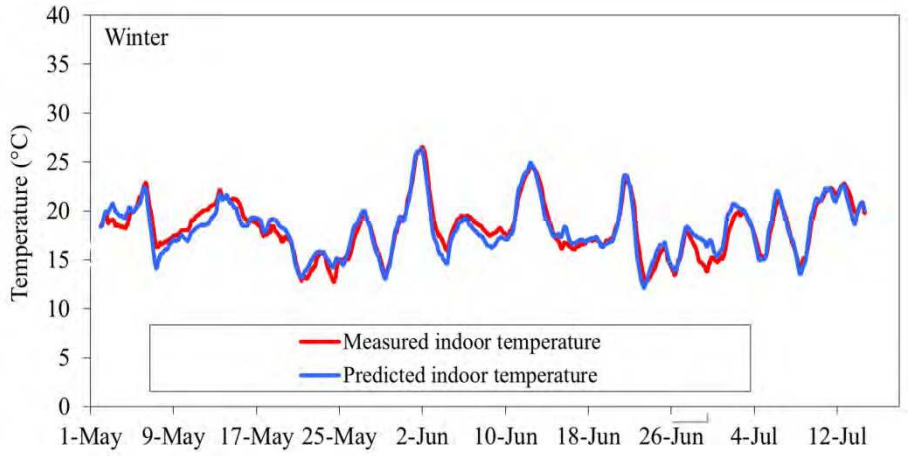

Fig. 17. Winter: Measured and predicted indoor temperature [Makaka, Meyer; 2011].

9. Conclusions

Fly ash bricks with the ratio 1:1 clay to fly ash mixing ratio were found to have the low water absorption, low thermal conductivity, high compressive strength and attractive decorative colour that eliminates the need for external plastering.

The monitoring results suggest that the building behaviour cannot be restricted to construction issues only. The thermal behaviour was the result of construction and non-construction factors, and their interaction as well.

Passive solar gain, ventilation mechanisms, orientation, and socio-environmental factors such as the life style and behaviour of the occupants, associated with the use of

complementary heating, operative heating (cooking, metabolic heat production), were found to have a significant impact on the indoor temperature distribution. The house performed differently in summer and winter. The indoor temperature followed the outdoor temperature implying that the solar radiation has a great impact on the indoor temperature variation.

The ventilation rate was found to depend on the ventilation component in use, windows were found to have a higher ventilation effect than doors. Correct opening and closing of windows can regulate the air infiltration thus controlling the indoor air quality.

When the day-to-day indoor temperature variations and the outdoor weather parameters are known, it is possible to reconstruct an approximate indoor temperature patterns during a given period. An indoor temperature prediction formula was modelled; it was shown that knowing the outdoor weather data parameters, the indoor temperature could be predicted. Outdoor temperature was found to have the largest impact on the indoor thermal environment. Significant differences were noted during cooking periods when a lot of heat was generated indoors, resulting in much higher measured indoor temperature than the model can predict. It is worth mentioning that the activities of the occupants play an important role in indoor temperature distribution.

10. References

[1] Agrement South Africa, (2002), Assessment criteria: Building and walling systems: Acoustics performance of buildings, http://www.agrement.co.za/.

[2] Kunzel, H. M, Zirkelbach, D. and Sedlbaur, (2003), Predicting indoor temperature and humidity conditions including hygrothermal interactions with the building envelope. Published in proceedings of the 1st International Conference on sustainable Energy and Green Architecture., Building Scientific Research Centre (BSRC), King Monkut's University Thornburi, Bangkoki 8-10 Oct. 2003.

[3] Makaka, G and Meyer, E. (2008), Thermal behaviour and ventilation efficiency of low-cost passive solar energy efficient house, Renewable energy 33 (2008), page 1959-1973

[4] Marsh, A., (2004), www.squ1.com

[5] Myers, E and George, F., (2004), Effect of ventilation rate and board loading on formaldehyde concentration: a critical review of literature. Forest products journal 2004, Vol. 34, number 10.

[6] Penman, R., (1982), Experimental determination of airflow in a naturally ventilated room using metabolic CO_2: Building and Environment, 17, 4.

[7] Raman, P., Mande, S. and Kishore, V. V. N., (2001), A passive solar system for thermal comfort conditioning of buildings in composite climates. Tata Energy Research Institute, Darbari Seth Block, Habitate place, Lodhi Road, New Delhi, India.

[8] Roulet, C. A., (1991), Simple and cheap air change rate measurement using CO_2 concentration decays. Air infiltration and ventilation centre Technical Note: 34.

[9] Wray, W., Balcomb, J.D., and Macfarland, R.D., (1979), A Semi Empirical method for estimating the performance of direct gain passive solar heated buildings. Proc. 3rd National Passive solar conference, San Jose California.

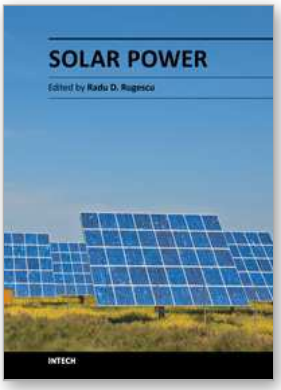

Solar Power

Edited by Prof. Radu Rugescu

ISBN 978-953-51-0014-0
Hard cover, 378 pages
Publisher InTech
Published online 15, February, 2012
Published in print edition February, 2012

A wide variety of detail regarding genuine and proprietary research from distinguished authors is presented, ranging from new means of evaluation of the local solar irradiance to the manufacturing technology of photovoltaic cells. Also included is the topic of biotechnology based on solar energy and electricity generation onboard space vehicles in an optimised manner with possible transfer to the Earth. The graphical material supports the presentation, transforming the reading into a pleasant and instructive labor for any interested specialist or student.

InTech Europe
University Campus STeP Ri
Slavka Krautzeka 83/A
51000 Rijeka, Croatia
Phone: +385 (51) 770 447
Fax: +385 (51) 686 166
www.intechopen.com

InTech China
Unit 405, Office Block, Hotel Equatorial Shanghai
No.65, Yan An Road (West), Shanghai, 200040, China
中国上海市延安西路65号上海国际贵都大饭店办公楼405单元
Phone: +86-21-62489820
Fax: +86-21-62489821